# SPURIOUS REFLECTION OF ELASTIC WAVES IN NONUNIFORM MESHES OF CONSTANT AND LINEAR STRAIN FINITE ELEMENTS

ZDENĚK P. BAŽANT† and ZEKAI CELEP‡

The Technological Institute, Northwestern University, Evanston, IL 60201, U.S.A.

**Abstract**—A change in finite element size causes spurious reflection of elastic waves passing through a finite element grid when the wavelength is less than about 10-times the largest element in the grid. Extending the previously published study in which the phenomenon was analyzed for the case of constant strain finite elements, the higher-order elements with linear strain distribution are studied herein. Similarly to the previous study, it is found that the consistent mass matrix gives less spurious wave reflection than the lumped mass matrix; however the advantage is smaller for the higher-order elements. For the lumped mass matrix, there is little difference in spurious wave reflection between the constant strain and linear strain elements. The phenomenon of spurious wave reflection is less pronounced when the higher-order elements are used in conjunction with the consistent mass matrix. These results are obtained from exact analytical solutions in complex variables for a planar wave with a planar wave front propagating along grid lines through an infinite grid which is uniform in each half plane.

## INTRODUCTION

A finite element grid is only an approximate representation of the continuum. One consequence of this fact is that elastic waves in a continuum cannot be faithfully represented by a finite element model. One of the limitations, to which attention has been recently called[1], is the inability of the finite element grid to transmit short wavelengths through an interface separating two half-planes in which the element sizes are uniform but different from each other. This problem has been analyzed in detail only for constant strain finite elements[1], for which the conditions of spurious reflection of elastic waves at the interface were rigorously formulated. From this analysis it is not clear, however, whether the spurious reflection phenomenon is the same for higher-order finite elements. Therefore, this study deals with the spurious reflection when higher-order finite elements are used. In particular, constant strain linear elements will be considered.

### REVIEW AND REFORMULATION OF SOLUTION FOR CONSTANT STRAIN ELEMENTS

Before approaching the problem of linear strain elements, as yet unsolved, it is appropriate to review the previous solution[1] for constant strain elements and at the same time reformulate it in a way which would be directly analogous to our subsequent solution for the linear strain element. We consider an infinite homogeneous elastic medium in which a longitudinal wave with a planar wave front propagates from left to right. Assuming the finite element grid to be uniform and rectangular, and the wave to propagate along the grid lines, the three-dimensional problem is equivalent to a one-dimensional problem for a series of line elements, each of which has two nodes (Fig. 1). We number the nodes consecutively as $k = \ldots, -3, -2, -1, 0, 1, 2, 3, \ldots$ and we assume that the element size at the left of point 0

is constant, denoted as $h$, and to the right of point 0 is also constant, denoted as $H$. Denoting the mass density of the continuum as $\rho$, we consider that the mass of the element is $m\rho h$ and that the nodes have an additional point mass $(1 - m)\rho h$. The case $m = 1$ corresponds to fully distributed mass, whereas the case $m = 0$ corresponds to lumping all the mass of the continuum into the nodes. The case $m = 1.5$ means that all mass is lumped into the centroid of the element, and values $m > 1.5$ are impossible. Referring to Fig. 1(c), the nodal forces acting on the $k$th element may be expressed as:

$$\left\{ \begin{matrix} F_k \\ F_{k+1} \end{matrix} \right\}_k = \frac{E}{h} \begin{bmatrix} 1 & -1 \\ -1 & 1 \end{bmatrix} \left\{ \begin{matrix} u_k \\ u_{k+1} \end{matrix} \right\} + \frac{m\rho h}{6} \begin{bmatrix} 2 & 1 \\ 1 & 2 \end{bmatrix} \left\{ \begin{matrix} \ddot{u}_k \\ \ddot{u}_{k+1} \end{matrix} \right\} \quad (1)$$

in which $u_k$ represents the displacement of the $k$th node to the right, and $E =$ Young's elastic modulus of the continuous medium. Expressing the dynamic equilibrium of nodal forces acting at node $k$ (Fig. 1e), we have

$$\frac{m}{6} \rho h (\ddot{u}_{k-1} + 4\ddot{u}_k + \ddot{u}_{k+1}) + (1 - m)\rho h \ddot{u}_k$$
$$= \frac{E}{h}(u_{k-1} - 2u_k + u_{k+1}). \quad (2)$$

In numerical computations we replace the time derivatives by the finite difference expression

$$\ddot{u}_k \simeq \frac{1}{\tau^2}(u_{k,r+1} - 2u_{k,r} + u_{k,r-1}) \quad (2a)$$

in which $\tau =$ time step, and $r =$ number of the time step. We seek the solution of eqns (2) and (2a) in form:

$$u_k(x, t) = e^{i\omega(x - vt)} + A e^{i\omega(-x - vt)} \quad (3)$$
$$= e^{i\omega(kh - v\tau r)} + A e^{i\omega(-kh - v\tau r)}$$

in which $i =$ imaginary unit, $\omega =$ circular frequency, $v =$ wave velocity. The first term in eqn (3) represents the incident wave, while the second term represents the

---

†Professor of Civil Engineering and Director, Center for Concrete and Geomaterials.
‡Post-Doctoral Research Associate, Associate Professor on leave from the Technical University, Istanbul.
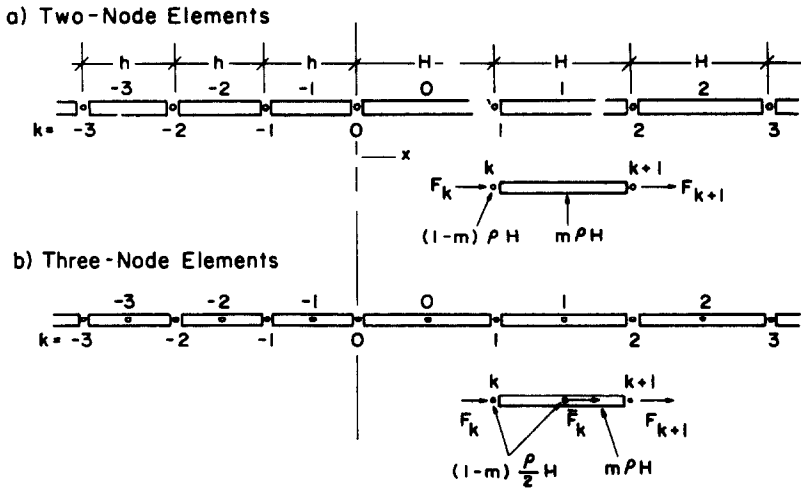
Fig. 1. Element numbering and notation.

reflected wave (if any). Substituting eqn (3) into eqn (2), we obtain:

$$\frac{v^2}{v_0^2}\left[1-m+\frac{m}{3}(2+\cos\omega h)\right]=\frac{\sin^2\dfrac{\omega h}{2}}{\dfrac{\omega^2 h^2}{4}}\cdot\frac{\dfrac{\omega^2 v^2\tau^2}{4}}{\sin^2\dfrac{\omega v\tau}{2}} \quad (4)$$

in which $v_0^2 = E/\rho$. One can check that $v^2 \to v_0^2$ for $h \to 0$ and $\tau \to 0$.

In case of a change in element size at $k = 0$, the equations with the foregoing notations are understood to apply to the left side of the grid ($k < 0$). For the right side ($k > 0$) we have the same solution but with a different complex amplitude $D$:

$$u_k = D\,e^{i\Omega(kH - V\tau\tau)} \quad (k \geq 0) \quad (5)$$

and similarly to eqn (4) we have for wave velocity:

$$\frac{V^2}{v_0^2}\left[1-m+\frac{m}{3}(2+\cos\Omega H)\right]=\frac{\sin^2\dfrac{\Omega H}{2}}{\dfrac{\Omega^2 H^2}{4}}\cdot\frac{\dfrac{\Omega^2 V^2\tau^2}{4}}{\sin^2\dfrac{\Omega V\tau}{2}}. \quad (6)$$

The quantities $V$, $\Omega$, and $H$ are analogous to $v$, $\omega$, $h$ and apply to the right side of the grid.

As the first interface condition, eqns (3) and (5) must yield the same displacement at $k = 0$; this gives:

$$e^{-i\omega v\tau\tau} + A\,e^{-i\omega v\tau\tau} = D\,e^{-i\Omega V\tau}. \quad (7)$$

Since this must hold for any time step $r$, we have

$$1 + A = D, \qquad \omega v = WV. \quad (8)$$

Using eqns (4), (6), and the second eqn (8), we obtain for the transmitted wave

$$\cos\Omega H = \frac{\left(\dfrac{H^2}{h^2}-1\right)[m(1-\cos\omega h)-3]+3\dfrac{H^2}{h^2}\cos\omega h}{m\left(\dfrac{H^2}{h^2}-1\right)(1-\cos\omega h)+3}. \quad (9)$$

One can check easily that $\Omega H \to \omega h$ for $H/h \to 1$. As the second interface condition, we must assure the balance of forces acting at node $k = 0$:

$$\frac{m}{6}\rho\,[h(\ddot{u}_{-1}+2\,\ddot{u}_0)+H(2\ddot{u}_0+u_1)]+(1-m)\rho\frac{h+H}{2}\ddot{u}_0$$

$$=\frac{E}{H}(u_1-u_0)-\frac{E}{h}(u_0-u_1). \quad (10)$$

By the same procedure as before we obtain

$$A\left\{\frac{m\omega^2 h^2 v^2}{3v_0^2}\left[2+Q+\frac{H}{h}(2+P)\right]\right.$$

$$+\frac{(1-m)\omega^2 h^2 v^2}{v_0^2}\left(1+\frac{H}{h}\right)$$

$$\left.+2\left[Q-1+\frac{h}{H}(P-1)\right]\frac{\dfrac{\omega^2 v^2\tau^2}{4}}{\sin^2\dfrac{\omega v\tau}{2}}\right\}$$

$$=2\frac{\dfrac{\omega^2 v^2\tau^2}{4}}{\sin^2\dfrac{\omega v\tau}{2}}\left[1-Q^{-1}+\frac{h}{H}(1-P)\right]$$

$$-\frac{m\omega^2 h^2 v^2}{3v_0^2}\left[Q^{-1}+2+\frac{H}{h}(P+2)\right]$$

$$-\frac{(1-m)\omega^2 h^2 v^2}{v_0^2}\left(1+\frac{H}{h}\right) \quad (11)$$

in which $Q = e^{i\omega h}$ and $P = e^{i\omega H}$. Introducing the real and imaginary parts as follows:

$$A = a_r + ia_i, \quad D = d_r + id_i$$

the relation $1 + A = D$ yields

$$1 + a_r = d_r; \qquad a_i = d_i. \quad (12)$$

For the real and imaginary parts of $A$ we obtain

$$a_r = \frac{TR + SZ\sin^2\omega h}{R^2 + S^2\sin^2\omega h}, \quad a_i = \frac{(RZ - TS)\sin\omega h}{R^2 + S^2\sin^2\omega h} \quad (13)$$

in which

$$R = \frac{m\omega^2 h^2 v^2}{v_0^2}\left[2 + \cos \omega h + \frac{H}{h}(2 + \cos \Omega H)\right.$$

$$+ \frac{(1-m)\omega^2 h^2 v^2}{v_0^2}\left(1 + \frac{H}{h}\right)$$

$$+ 2\left[\cos \omega h - 1 + \frac{h}{H}(\cos \omega H - 1)\right]\frac{\frac{\omega^2 v^2 \tau^2}{4}}{\sin^2 \frac{\omega v \tau}{2}}$$

$$S = \frac{m\omega^2 h^2 v^2}{3v_0^2}\left(1 + \frac{H}{h}\frac{\sin \Omega H}{\sin \omega h}\right)$$

$$+ 2\left(1 + \frac{h}{H}\frac{\sin \Omega H}{\sin \omega h}\right)\frac{\frac{\omega^2 v^2 \tau^2}{4}}{\sin^2 \frac{\omega v \tau}{2}} \tag{14}$$

$$T = -R$$

$$Z = \frac{m\omega^2 h^2 v^2}{3v_0^2}\left(1 - \frac{H}{h}\frac{\sin \Omega H}{\sin \omega h}\right)$$

$$+ 2\left(1 - \frac{h}{H}\frac{\sin \Omega H}{\sin \omega h}\right)\frac{\frac{\omega^2 v^2 \tau^2}{4}}{\sin^2 \frac{\omega v \tau}{2}}.$$

Similarly to the previous work[1], the energy flux to the right may be expressed as:

$$\mathcal{P} = \text{Re}\,(F_k)\,\text{Re}\,(u_k) \tag{15}$$

which reduces to the expression

$$\mathcal{P} = \left[\frac{E}{h}\text{Re}\,(u_k - u_{k-1}) + \frac{m\rho h}{6}\text{Re}\,(2\ddot{u}_k + \ddot{u}_{k-1})\right]\text{Re}\,(u_k). \tag{16}$$

Denoting $\mathcal{P}_1$, $\mathcal{P}_A$ and $\mathcal{P}_D$ the energy fluxes of the incident wave, the reflected wave, and the transmitted wave, we obtain for the time-average energy fluxes:

$$\langle\mathcal{P}_1\rangle = -\frac{\pi E}{h}\left(1 + \frac{m\omega^2 h^2}{6}\frac{v^2}{v_0^2}\right)\sin \omega h \quad (\text{incident} \rightarrow)$$

$$\langle\mathcal{P}_A\rangle = \frac{\pi E}{h}\left(1 + \frac{m\omega^2 h^2}{6}\frac{v^2}{v_0^2}\right)$$

$$\times (a_r^2 + a_i^2)\sin \omega h \qquad (\text{reflected} \leftarrow) \tag{17}$$

$$\langle\mathcal{P}_D\rangle = -\frac{\pi E}{H}\left(1 + \frac{m\Omega^2 H^2}{6}\frac{V^2}{v_0^2}\right) \qquad (\text{refracted} \rightarrow).$$

$$\times (d_r^2 + d_i^2)\sin \Omega H$$

One can check that these time-average fluxes always satisfy the relation

$$\langle\mathcal{P}_1\rangle = \langle\mathcal{P}_A\rangle + \langle\mathcal{P}_D\rangle \tag{18}$$

required for conservation of energy.

## SOLUTION FOR THREE-NODE LINE ELEMENTS OF LINEAR STRAIN DISTRIBUTION

We now consider three-node line elements keeping node numbers $k$ reserved for the boundary nodes of elements; see Fig. 1(d). At the same time we use $k$ to number the finite elements, in which case $k$ also refers to the interior node (Fig. 1d). The mass of the element is again $m\rho h$. Since there are three nodal points at element, the mass at each nodal point now is $(1 - m)\rho h/2$. The nodal forces acting on the $k$th finite element (Fig. 1e) are characterized by

$$\begin{bmatrix} F_k \\ \bar{F}_k \\ F_{k+1} \end{bmatrix}_k = \frac{E}{3h}\begin{bmatrix} 7 & -8 & 1 \\ -8 & 16 & -8 \\ 1 & -8 & 7 \end{bmatrix}\begin{Bmatrix} u_k \\ v_k \\ u_{k+1} \end{Bmatrix}$$

$$+ \frac{m\rho h}{30}\begin{bmatrix} 4 & 2 & -1 \\ 2 & 16 & 2 \\ -1 & 2 & 4 \end{bmatrix}\begin{Bmatrix} \ddot{u}_k \\ \ddot{v}_k \\ \ddot{u}_{k+1} \end{Bmatrix} \tag{19}$$

in which $\bar{F}_k$ denotes the force acting from the interior node, $u_k$ denotes the displacements of the boundary nodes, and $v_k$ denotes the dipplacement of the interior node of the $k$th element. The equation of motion at element boundary node $k$ is

$$(1 - m)\frac{\rho h}{2}\ddot{u}_k + \frac{m\rho h}{30}(-\ddot{u}_{k-1} + 2\ddot{v}_{k-1} + 8\ddot{u}_k + 2\ddot{v}_k - \ddot{u}_{k+1})$$

$$= \frac{E}{3h}(-u_{k-1} + 8v_{k-1} - 14u_k + 8v_k - u_{k+1}) \tag{20}$$

and the equation of motion at the interior nodal point of the $k$th element is

$$(1 - m)\frac{\rho h}{2}\ddot{v}_k + \frac{m\rho h}{15}(\ddot{u}_k + 8\ddot{v}_k + \ddot{u}_{k+1})$$

$$= \frac{8E}{3h}(u_k - 2v_k + u_{k+1}). \tag{21}$$

The solutions of eqns (20), (21) with expressions in eqn (2a) may be sought in the form:

$$u_k = e^{i\omega(kh - v\tau\tau)} + A\,e^{i\omega(-kh - v\tau\tau)}$$

$$v_k = B\,e^{i\omega[(k+1/2)h - v\tau\tau)]} + C\,e^{i\omega[-(k+1/2)h - v\tau\tau]}. \tag{22}$$

Substituting these expressions into eqns (20) and (21) gives

$$au_k = b(v_{k-1} + v_k), \quad cv_k = b(u_k + u_{k+1}) \tag{23}$$

in which

$$a = \frac{2}{3}(\cos \omega h + 7) - \frac{\sin^2 \frac{\omega v \tau}{2}}{\frac{\omega^2 v^2 \tau^2}{4}}$$

$$\times \omega^2 h^2 \frac{v^2}{v_0^2}\left[\frac{m}{15}(4 - \cos \omega h) + \frac{1-m}{2}\right]$$

$$b = \frac{8}{3} + \frac{\sin^2 \frac{\omega v \tau}{2}}{\frac{\omega^2 v^2 \tau^2}{4}}\omega^2 h^2 \frac{v^2}{v_0^2}\frac{m}{15}$$

$$c = \frac{16}{3} - \frac{\sin^2 \frac{\omega v \tau}{2}}{\frac{\omega^2 v^2 \tau^2}{4}}\omega^2 h^2 \frac{v^2}{v_0^2}\left(\frac{8m}{15} + \frac{1-m}{2}\right). \tag{24}$$

Using the last two equations, we may obtain the following relation

$$ac = 2b^2(1 + \cos \omega h) \tag{25}$$

from which the wave velocity $v$ can be solved.

If the element size $H$ for the right side of the grid differs from the size $h$ for the left side, we must rewrite the equation of motion (eqn 20) replacing $h$ with $H$ and substituting the solution for the transmitted wave in the form

$$u_k = D e^{i\Omega(kH - V\tau)}, \quad v_k = E\, e^{i\Omega[(k+1/2)H - V\tau]} \quad (k \ge 0) \tag{26}$$

we get the relations

$$\bar{a} u_k = \bar{b}(v_{k-1} + v_k), \quad \bar{c} v_k = \bar{b}(u_k + u_{k+1}) \tag{27}$$

in which $\bar{a}$, $\bar{b}$ and $\bar{c}$ are expressed in the same way as eqn (24) except that $\omega$, $h$ and $v$ must now be replaced with $\Omega$, $H$ and $V$. Similarly to eqn (6) we may also verify the relation

$$\bar{a}\bar{c} = 2\bar{b}^2 (1 + \cos \Omega H) \tag{28}$$

from which the velocity of the transmitted wave $V$ may be solved.

The interface condition of equal displacement at $k = 0$ requires

$$e^{-i\omega v\tau} + A\, e^{-i\omega v\tau} = D\, e^{-i\omega V\tau}. \tag{29}$$

This may be reduced to

$$1 + A = D \quad \text{or} \quad 1 + a_r = d_r, \quad a_i = d_i \tag{30}$$

$$\omega v = \Omega V. \tag{31}$$

Now, using eqns (4), (6) and (8) we obtain for the transmitted wave

$$\cos \Omega H = \frac{h_1 h_2 - 2 h_3^2}{2 h_3^2 - h_1 h_4} \tag{32}$$

in which

$$h_1 = \frac{16}{3} - \frac{\sin^2 \frac{\omega v\tau}{2}}{\frac{\omega^2 v^2 \tau^2}{4}} \omega^2 h^2 \frac{v^2}{v_0^2} \frac{H^2}{h^2} \left( \frac{8m}{15} + \frac{1+m}{2} \right)$$

$$h_2 = \frac{14}{3} - \frac{\sin^2 \frac{\omega v\tau}{2}}{\frac{\omega^2 v^2 \tau^2}{4}} \omega^2 h^2 \frac{v^2}{v_0^2} \frac{H^2}{h^2} \left( \frac{4m}{15} + \frac{1-m}{2} \right)$$

$$h_3 = \frac{8}{3} + \omega^2 h^2 \frac{v^2}{v_0^2} \frac{H^2}{h^2} \frac{m}{15} \frac{\sin^2 \frac{\omega v\tau}{2}}{\frac{\omega^2 v^2 \tau^2}{4}}$$

$$h_4 = \frac{2}{3} + \frac{\sin^2 \frac{\omega v\tau}{2}}{\frac{\omega^2 v^2 \tau^2}{4}} \omega^2 h^2 \frac{v^2}{v_0^2} \frac{H^2}{h^2} \frac{m}{15}. \tag{33}$$

Substituting eqn (23) into eqn (22), we further obtain two relations between the complex amplitudes $A$, $B$ and $C$:

$$B = 2\frac{b}{c} \cos \frac{\omega h}{2}, \quad C = 2A\frac{b}{c} \cos \frac{\omega h}{2}. \tag{34}$$

In terms of the real and imaginary parts, these are equivalent to:

$$b_r = 2\frac{b}{c} \cos \frac{\omega h}{2}, \quad b_i = 0;$$

$$c_r = 2a_r \frac{b}{c} \cos \frac{\omega h}{2}, \quad c_i = 2a_i \frac{b}{a} \cos \frac{\omega h}{2} \tag{35}$$

in which $C = c_r + i c_i$, $B = b_r + i b_i$.

Using eqns (29) and (30), we may obtain similar equations for the right side of the grid $(k \ge 0)$:

$$E = 2D\frac{\bar{b}}{\bar{c}} \cos \frac{\Omega H}{2} \tag{36}$$

or

$$e_r = 2d_r \frac{\bar{b}}{\bar{c}} \cos \frac{\Omega H}{2}; \quad e_i = 2d_i \frac{\bar{b}}{\bar{c}} \cos \frac{\Omega H}{2}. \tag{37}$$

As the second interface condition, the force balance at node $k = 0$ requires that

$$(1 - m)\frac{\rho}{4}(h + H)\ddot{u}_0$$

$$+ \frac{m\rho}{30}[h(-\ddot{u}_{-1} + 2\ddot{v}_{-1} + 4\ddot{u}_0) + H(4\ddot{u}_0 + 2\ddot{v}_0 - \ddot{u}_1)] \tag{38}$$

$$= \frac{E}{3h}(-u_{-1} + 8v_{-1} - 7u_0) + \frac{E}{3H}(-7u_0 + 8v_0 - u_1).$$

After some manipulations this yields

$$A \left\{ \frac{m^2 \omega^2 h^2 v^2}{30 v_0^2} \left[ 4 - Q + \frac{H}{h}(4 - P) + 4\frac{b}{c} Q^{1/2} \cos \frac{\omega h}{2} \right. \right.$$

$$\left. + 4\frac{H}{h}\frac{\bar{b}}{\bar{c}} P^{1/2} \cos \frac{\Omega H}{2} \right] + \frac{(1-m)\omega^2 h^2 v^2}{4 v_0^2} \left( 1 + \frac{H}{h} \right)$$

$$+ \frac{1}{3} \left[ 16\frac{b}{c} Q^{1/2} \cos \frac{\omega h}{2} + 16\frac{h}{H}\frac{\bar{b}}{\bar{c}} P^{1/2} \cos \frac{\Omega H}{2} - (7 + Q) \right.$$

$$\left. \left. - \frac{h}{H}(7 + P) \right] \frac{\frac{\omega^2 v^2 \tau^2}{4}}{\sin^2 \frac{\omega v\tau}{2}} \right\} \tag{39}$$

$$= \frac{1}{3} \frac{\frac{\omega^2 v^2 \tau^2}{4}}{\sin^2 \frac{\omega v\tau}{2}} \left[ 7 + Q^{-1} + \frac{h}{H}(7 + P) - 16\frac{b}{c} Q^{-1/2} \cos \frac{\omega h}{2} \right.$$

$$\left. - 16\frac{h}{H}\frac{\bar{b}}{\bar{c}} P^{1/2} \cos \frac{\Omega H}{2} \right] - \frac{m\omega^2 h^2 v^2}{30 v_0^2} \left[ 4 - Q^{-1} \right.$$

$$\left. + \frac{H}{h}(4 - P) + 4\frac{b}{c} Q^{-1/2} \cos \frac{\omega h}{2} + 4\frac{H}{h}\frac{\bar{b}}{\bar{c}} P^{1/2} \cos \frac{\Omega H}{2} \right]$$

$$- \frac{(1-m)\omega^2 h^2 v^2}{v_0^2} \left( 1 + \frac{H}{h} \right).$$

Splitting $A$ in the real and imaginary parts, $A = a_r + i\, a_i$, we get

$$a_r = \frac{TR + SZ \sin^2 \omega h}{R^2 + S^2 \sin^2 \omega h}, \quad a_i = \frac{(RZ - TS) \sin \omega h}{R^2 + S^2 \sin \omega h} \quad (40)$$

in which

$$R = \frac{m\omega^2 h^2 v^2}{30 v_0^2} \left[ 4 - \cos \omega h + \frac{H}{h}(4 - \cos \Omega H) \right.$$

$$\left. + 4\frac{b}{c}\cos^2\frac{\omega h}{2} + 4\frac{H}{h}\frac{\bar{b}}{\bar{c}}\cos^2\frac{\Omega H}{2} \right]$$

$$+ \frac{(1-m)\omega^2 h^2 v^2}{4 v_0^2}\left(1 + \frac{H}{h}\right)$$

$$+ \frac{1}{3}\left[ \left( 16\frac{b}{c}\cos^2\frac{\omega h}{2} - 7 - \cos \omega h \right) \right.$$

$$\left. + \frac{h}{H}\left( 16\frac{\bar{b}}{\bar{c}}\cos^2\frac{\Omega H}{2} - 7 - \cos \Omega H \right) \right]\frac{\frac{\omega^2 v^2 \tau^2}{4}}{\sin^2\frac{\omega v \tau}{2}}, \quad (41)$$

$$S = \frac{m\omega^2 h^2 v^2}{30 v_0^2}\left[ 2\frac{b}{c} - 1 + \frac{H}{h}\left( 2\frac{\bar{b}}{\bar{c}} - 1 \right)\frac{\sin \Omega H}{\sin \omega h} \right]$$

$$+ \frac{1}{3}\left[ 8\frac{b}{c} - 1 + \frac{h}{H}\left( 8\frac{\bar{b}}{\bar{c}} - 1 \right)\frac{\sin \Omega H}{m\omega h} \right]\frac{\frac{\omega^2 v^2 \tau^2}{4}}{\sin^2\frac{\omega v \tau}{2}}$$

$$T = -R,$$

$$Z = -\frac{m\omega^2 h^2 v^2}{30 v_0^2}\left[ 1 - 2\frac{b}{c} - \frac{H}{h}\left( 1 - 2\frac{\bar{b}}{\bar{c}} \right)\frac{\sin \Omega H}{\sin \omega h} \right]$$

$$- \frac{1}{3}\left[ 1 - 8\frac{b}{c} - \frac{h}{H}\left( 1 - 8\frac{\bar{b}}{\bar{c}} \right)\frac{\sin \Omega H}{\sin \omega h} \right]\frac{\frac{\omega^2 v^2 \tau^2}{4}}{\sin^2\frac{\omega v \tau}{2}}.$$

The energy flux to the right may now be expressed as

$$\mathcal{P} = \left[ \frac{E}{h}\,\mathrm{Re}\,(u_{k-1} - 8v_{k-1} + 7u_k) \right.$$

$$\left. + \frac{m\rho h}{30}\,\mathrm{Re}\,(-\ddot{u}_{k-1} + 2\ddot{v}_{k-1} + 4\ddot{u}_k) \right]\mathrm{Re}\,(u_k). \quad (42)$$

Taking the time-average fluxes, we obtain
Incident wave:

$$\langle \mathcal{P}_1 \rangle = -\frac{\pi E}{3h}\left\{ 8b_r \sin\frac{\omega h}{2} - \sin \omega h \right.$$

$$\left. + \frac{m\omega^2 h^2}{10}\frac{v^2}{v_0^2}\left[ 2b_r \sin\frac{\omega h}{2} - \sin \omega h \right] \right\}. \quad (43)$$

Reflected wave:

$$\langle \mathcal{P}_A \rangle = \frac{\pi E}{3h}\left\{ 8(a_r c_r + a_i c_i)\sin\frac{\omega h}{2} \right.$$

$$+ 8(a_r c_i - a_i c_r)\cos\frac{\omega h}{2} - (a_r^2 + a_i^2)\sin \omega h$$

$$+ \frac{m\omega^2 h^2}{10}\frac{v^2}{v_0^2}\left[ 2(a_r c_r + a_i c_i)\sin\frac{\omega h}{2} + 2(a_r c_i - a_i c_r) \right.$$

$$\left. \cos\frac{\omega h}{2} - (a_r^2 + a_i^2)\sin \omega h \right] \bigg\}.$$

Diffracted wave:

$$\langle \mathcal{P}_D \rangle = -\frac{\pi E}{3H}\left\{ 8(d_r e_r + d_i e_i)\sin\frac{\Omega H}{2} \right.$$

$$- 8(d_r e_i - d_i e_r)\cos\frac{\Omega H}{2} - (d_r^2 + d_i^2)\sin \Omega H$$

$$+ \frac{m\Omega^2 H^2}{10}\frac{V^2}{v_0^2}\left[ 2(d_r e_r + d_i e_i)\sin\frac{\Omega H}{2} \right.$$

$$\left. - 2(d_r e_i - d_i e_r)\cos\frac{\Omega H}{2} - (d_r^2 + d_i^2)\sin \Omega H \right] \bigg\}.$$

With this we obtained all information of interest for the wave diffraction in the grid.

## NUMERICAL RESULTS

Figure 2(a) shows the variation of the relative wave velocity in the grid, $v/v_0$, with the relative wavelength $l/h$ for the constant strain finite elements (elements having two nodes), the wavelengths being obtained as $l = 2\pi/\omega$. Figure 2(b) shows the same for the finite elements with linear strain variation (elements having three nodes). These plots were obtained from eqn (4) for various values of $m$ and for an infinitely short time-step ($\tau = 0$). Note that $v/v_0 = 0$ for $l/h = 1$, and that $v/v_0 > 1$ for $l/h = \infty$. Comparison of Figs. 2 (a, b) indicates that for the higher-order elements (linear strain distribution) the effect of the mass distribution parameter $m$ is much less than it is for the lower-order elements (constant strain distribution). Figure 2 (c, b) illustrates the same relations in greater detail in the vicinity of $v/v_0 = 1$.

The characteristic quantity $\Omega H$ can be solved from eqn (32). The solution exists if, and only if, $-1 \leq \cos \Omega H \leq 1$. The solution gives a relation between $H/h$ and the quantity $\omega h = 2\pi(l/h)$, which is shown in Figs. 3 (a, b). The combinations of $l/h$ and $H/h$ values below the curves satisfy the foregoing inequality and yield a solution for the transmitted wave, whereas the values above these curves do not satisfy the foregoing inequality. Note that for the case of two-node elements (constant strain) the value $m = 1.5$ gives always a solution except when $l/h = 2$.

The graphs of the transmitted wave velocity $V$ relative to the wave velocity $v_0$ of the continuous medium are shown in Figs. 4 (a, b). The end points of the curves correspond to the case $|\cos \Omega H| = 1$. Figure 4(a, b) pertain to $l/h = 4$. The same curves for $l/h = 6$ are shown in Figs. 4 (c, d).

The amplitude and the energy flux of the spurious reflected wave are plotted in Figs. 5 (a, b) for the case of two-node elements. Note that for $m = 1.5$ there is no reflected wave. The larger is $H/h$, the greater is the energy of the reflected wave. For a certain value of $H/h$, the entire energy flux is reflected and there is no transmitted wave, i.e. $\cos \Omega H = 1$. In that case, as expected, the amplitude of the reflected wave equals the amplitude of the incoming wave. Figure 5(a) corresponds to two-node elements and Fig. 5(b) to three-node elements. Note that the curves for three-node elements are similar for $m = 0$, 0.25 and 0.50. But for $m = 0.75$ there exists a certain value of $H/h$ for which there is no reflected wave. Furthermore, for $m = 1.0$ and $m = 1.5$ the sign of $A$ is opposite (this is also true for $m = 0.75$). Figures 5 (a, b) refers to $l/h = 4$. The same results for $l/h = 6$ are plotted in Figs. 5 (c, d).
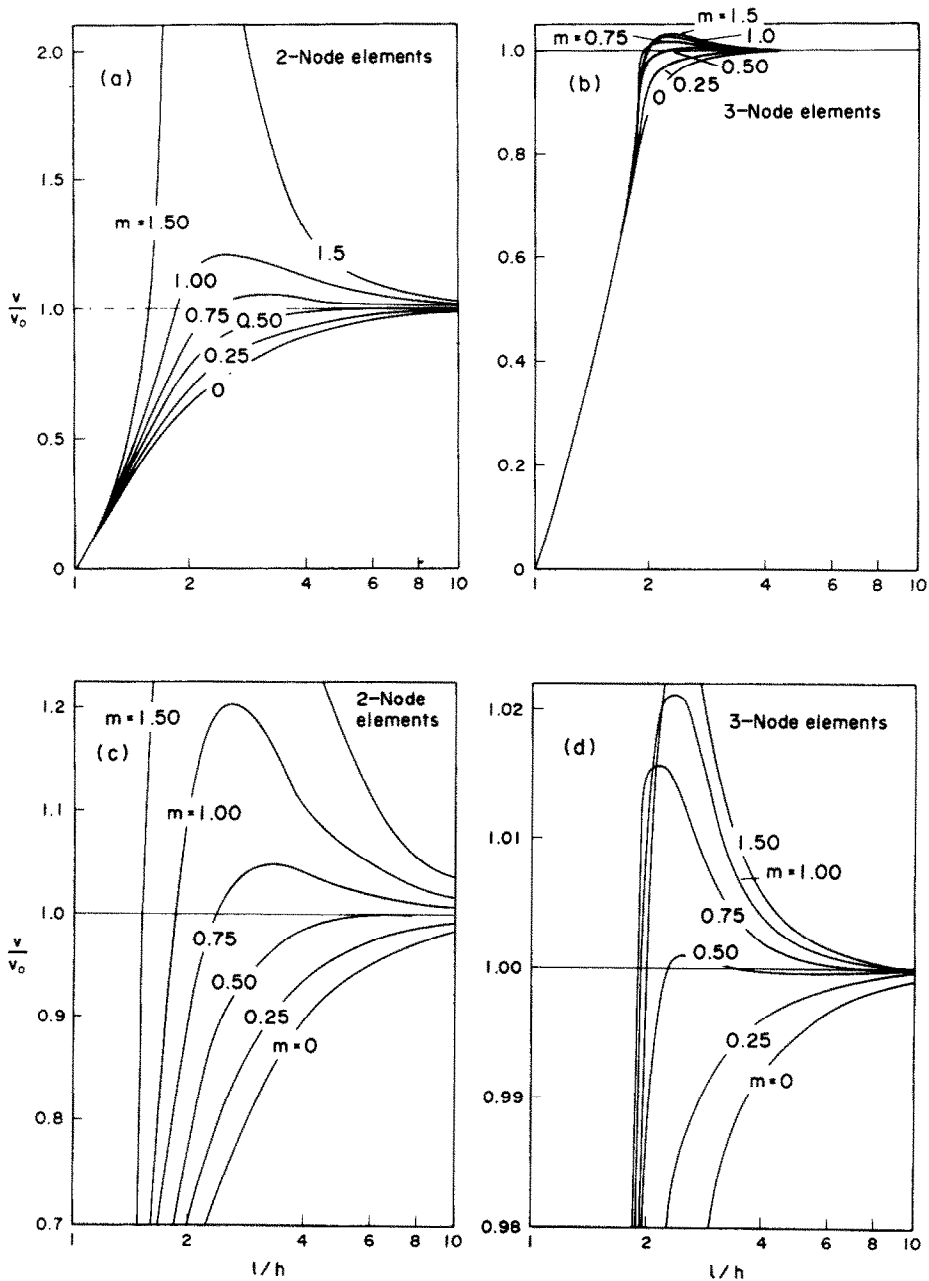
Fig. 2. Variation of relative wave velocity with relative wavelength.

The results for two-node elements confirm the conclusions of Ref. [1]. The spurious reflection is significant when $L$ is less than about $10H$ for lumped mass and $L$ is less than about $6H$ for consistent mass. The only way to avoid the spurious reflection is either to use a uniform grid or to filter out in the input or at the output the shortest wavelengths (the highest frequencies). Within the range of normal time steps that would be used in explicit integration algorithms, the magnitude of the time step has a negligible effect on spurious wave reflection. For this reason we show here only the results for $\tau = 0$.

As far as the spurious wave reflection is concerned, the consistent mass matrix performs better than the lumped mass matrix. This advantage of the consistent mass matrix contrasts with the fact that the lumped mass matrix is superior in terms of numerical statility as well as spurious high-frequency oscillations of the grid, and that for the wave dispersion a combination of the lumped and consistent mass matrices is preferable to either one of them. The choice between these matrices thus depends on which aspect is more important in a given problem.
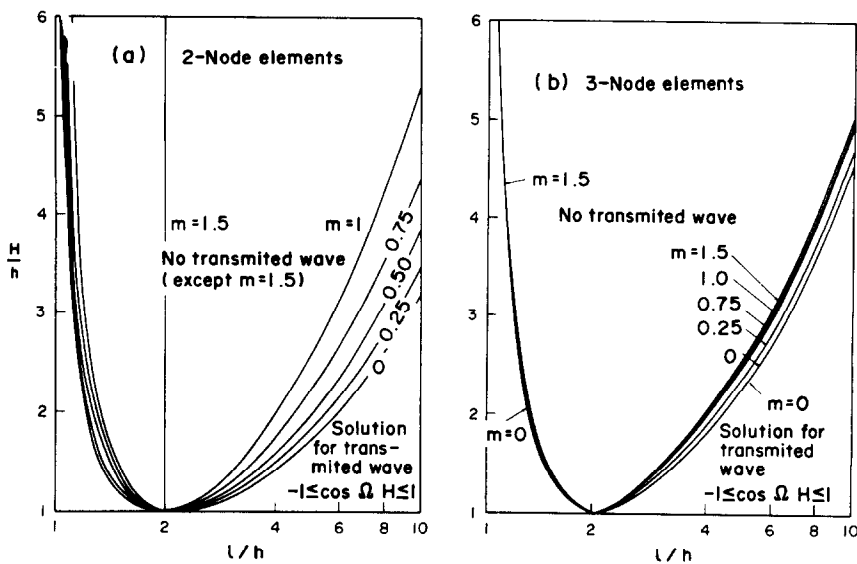
Fig. 3. Maximum element-size ratio for which transmitted wave exists at various wavelength.
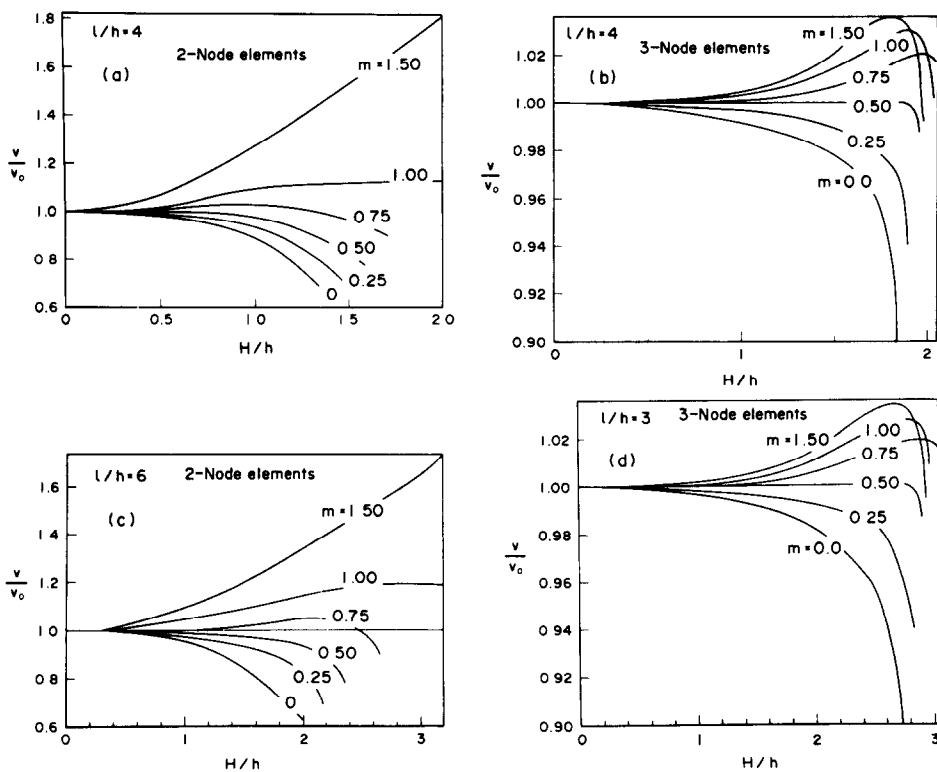


Fig. 4. Relative velocity of transmitted wave as a function of element size ratio.
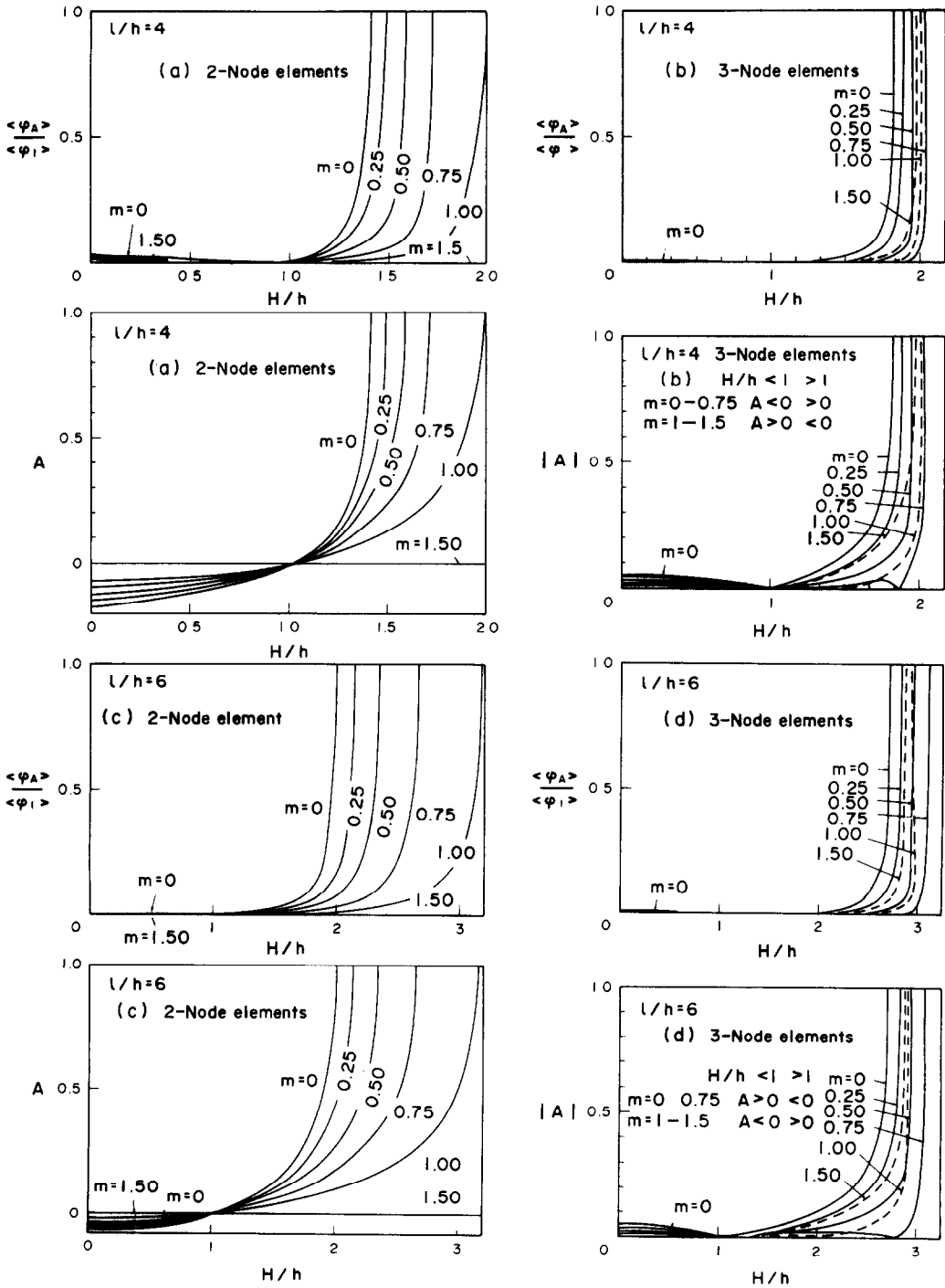
Fig. 5. Energy flux and amplitude of spurious reflected wave as a function of element size ratio.

## CONCLUSIONS

The purpose of this study has been to extend the analysis from Ref. [1] by comparing the spurious reflection for grids consisting of constant strain elements and linear strain elements. In this respect the following conclusions may be drawn:

(1) The advantage of the consistent mass matrix over the lumped mass matrix in terms of the spurious wave reflection becomes smaller for the higher-order elements (linear strain distribution).

(2) The spurious wave reflection for the lumped mass matrix is about equally pronounced for the lower- and higher-order finite elements (constant strain and linear strain).

(3) The problems of the spurious wave reflection are less severe for the higher-order elements, i.e. a higher difference between element sizes is needed to achieve the same percentage of reflection of energy flux. This difference is more marked for the consistent mass matrix.

## REFERENCE

1. Z. P. Bažant, Spurious reflection of elastic waves in nonuniform finite element grids. *Comput. Meth. in Appl. Mech. and Engng*, 16, 91–100 (1978).